



# Online Identification of a Mechanical System in the Frequency Domain with Short-Time DFT

N.Nevaranta J.Parkkinen T.Lindh M.Niemelä O.Pyrhönen J.Pyrhönen

*Department of Electrical Engineering, Lappeenranta University of Technology, FI-53851 Lappeenranta, Finland.  
E-mail: {Niko.Nevaranta,Jukka.Parkkinen,Tuomo.Lindh,Markku.Niemela,Olli.Pyrhonen,Juha.Pyrhonen}@lut.fi*

---

## Abstract

A proper system identification method is of great importance in the process of acquiring an analytical model that adequately represents the characteristics of the monitored system. While the use of different time-domain online identification techniques has been widely recognized as a powerful approach for system diagnostics, the frequency domain identification techniques have primarily been considered for offline commissioning purposes. This paper addresses issues in the online frequency domain identification of a flexible two-mass mechanical system with varying dynamics, and a particular attention is paid to detect the changes in the system dynamics. An online identification method is presented that is based on a recursive Kalman filter configured to perform like a discrete Fourier transform (DFT) at a selected set of frequencies. The experimental online identification results are compared with the corresponding values obtained from the offline-identified frequency responses. The results show an acceptable agreement and demonstrate the feasibility of the proposed identification method.

*Keywords:* Kalman filter, Nonparametric estimation, Online identification, Short-time DFT, Two-mass system

---

## 1 Introduction

The identification of a mechanical system in electric drives has become an increasingly important feature in different high-performance motion control applications such as robotics, machine tools, material handling, and packaging, to name but a few. As the control performance plays an important role in these applications, the increasing demand for high reliability significantly motivates to improve the methods, tools, and techniques for the diagnostics and condition monitoring of a mechanical system. The deterioration of mechanical parts over time or other unexpected changes in the system dynamics may lead to degradation of the control performance. These adverse effects can cause unexpected interruptions to the production processes, for example, in material handling. Thus, it is important to detect the system changes as proactive main-

tenance before they lead to performance degradation, which could eventually lead to production losses. For these reasons, different system identification techniques for the condition monitoring of mechanical parts are viable methods to enhance the reliability of electrical drives.

In the literature there are numerous papers describing identification techniques for different mechanical systems. In general, a mechanical system can be identified either in the offline or in online mode by time- or frequency-domain observations. Broadly speaking, traditional identification techniques can be divided into two main categories: nonparametric estimation methods (Villwock and Pacas, 2008), (Wang et al., 2011), (Ruderman, 2014) and parametric estimation methods (Saarakkala and Hinkkanen, 2013). For commissioning purposes, frequency-domain offline identification techniques are widely recognized, and they have been

successfully applied to parameter estimation of different mechanical systems in closed-loop control (Beineke et al., 1998), (Beck and Turschner, 2001). Correspondingly, other studies have considered the closed-loop time-domain identification of mechanical systems for parameter estimation and control design purposes (Saarakkala and Hinkkanen, 2013), (Nevaranta et al., 2013), (Calvini et al., 2015). Especially, recent advances in time-domain prediction error approaches (Toth et al., 2012) have mitigated the closed-loop issues. Some of these methods have been successfully applied to online parameter estimation by considering their recursive form (Nevaranta et al., 2015), (Garrido and Concha, 2013). For online identification purposes, recursive time-domain parameter estimation methods have received the most attention as they have been shown to overcome many of the drawbacks of classical frequency-domain techniques in terms of closed-loop issues, accuracy, computational cost, and memory storage requirements.

Despite the above theoretical development, there are hardly any studies available on the issues related to the use of frequency-domain techniques for online system identification. As the computational capacity has increased, the real-time frequency domain techniques could introduce attractive features for example for the online monitoring of a mechanical system at a selected set of frequencies. In (Morelli, 2000), a real-time equation error method based on finite Fourier transform in the frequency domain is used for linear model identification. Another approach has been reported in (Jenssen and Zarrop, 1994), where a recursive Kalman filter is configured to perform like a Fourier transform (Bitmead et al., 1986). These methods are regarded as a short-time discrete Fourier transform. In (LaMaire et al., 1987), (Kurita et al., 1999) adaptive frequency domain online identification based control law have been proposed. Furthermore, other frequency domain identification methods used in real-time have been reported in (Barkley and Santi, 2009). However, these methods have high memory storage requirements for data acquisition (Kurita et al., 1999) or take an iterative form (Barkley and Santi, 2009).

Even though several studies have applied different online and offline methods to identify the dynamics of the mechanical parts, to the authors knowledge, none of the previous studies have discussed or considered online identification of a mechanical system in the frequency domain. In practice, the advantages of frequency domain techniques based on a Fourier transform are that the bias and drift are removed from the measured data. Secondly, by using a priori knowledge of the expected frequency range, that is, a selected set of frequencies of the excitation signal, the data to be

analyzed can be easily reduced. Motivated by the features of the short-time DFT algorithm in (Jenssen and Zarrop, 1994), (Bitmead et al., 1986), (Kamwa et al., 2014), the objective of this paper is to study online nonparametric identification of the frequency response in selected frequency points and monitoring of a velocity-controlled two-mass-system in a closed-loop control. In particular, the main idea of using the short-time DFT for identification purposes presented in (Jenssen and Zarrop, 1994) is considered, but here the theory is supported by measurement results, and the identification is carried out in a different manner. The direct identification is considered by using the measured input and output signals.

This paper studies an example case of the frequency-domain online identification of a two-mass-system. The system under study is a coupled belt system with mechanical dynamics consisting of two moments of inertias coupled by flexible belt material. The online identification is performed by exciting the system with a multi-sine excitation signal and using a short-time DFT. In the approach, nonparametric identification is performed at a selected set of frequencies that are chosen from the offline-identified frequency response and prior knowledge of the system dynamics. For validation purposes, the system dynamics of the experimental test setup is varied by changing the belt material in the system. Furthermore, the normalized Vinnicombe gap metric is used as an illustrative distance metric in order to compare offline- and online-identified models in the desired frequency range when the system has been modified.

The contents of the paper are organized as follows. First, a mathematical model of the flexible belt system under consideration is developed and introduced in Section 2. After that, the online identification procedure for the mechanical system under study is introduced in Section 3. Finally, the experimental test setup is presented and identification results are shown and analyzed in Section 4. Section 5 concludes the paper.

## 2 Model of the Two-mass-system

The investigated two-mass-system is a coupled belt system with mechanical dynamics consisting of two moments of inertias coupled by flexible belt material as depicted in Figure 1. The dynamics of the mechanical system in Figure 1 can be described by the following set of equations

$$J_1 \frac{d\Omega_1}{dt} = T_1 - T_{fr1} + r_1 F \quad (1)$$

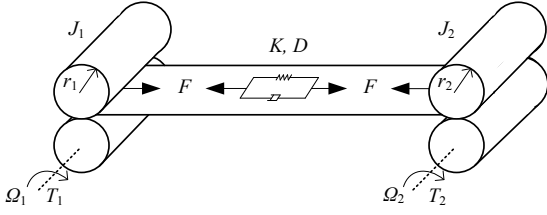


Figure 1: Flexible two-mass-system

$$J_2 \frac{d\Omega_2}{dt} = T_2 - T_{fr} - r_2 F \quad (2)$$

$$F = K(r_2 \Omega_2 - r_1 \Omega_1) + D(r_2 \dot{\Omega}_2 - r_1 \dot{\Omega}_1) \quad (3)$$

Equations (1) and (2) are the elementary dynamic equations for rotation, where  $J$  is the moment of inertia,  $\Omega$  is the angular velocity,  $T$  is the torque,  $T_{fr}$  is the frictional torque component,  $r$  is the roller radius, and  $F$  represents the tension force. The dynamics of the coupling is expressed by (3), where  $K$  is the spring constant and  $D$  is the damping constant of the belt material. In this paper, the dynamics of the two-mass-system is modified in order to show the applicability of the proposed identification method. The reference models for the system under study are calculated from the material properties and the geometrical values presented in Table 1. The reference models are used to compare the experimentally identified models. It is pointed out that the original parameters of the experimental test setup, especially the belt properties, are only known with some degree of confidence.

### 3 Short-Time DFT

The standard method for spectrum analysis is the discrete Fourier transform, which, in practice, requires an  $N$  array of samples. For real-time implementation, a recursive Kalman filter can be configured to perform like a Fourier transform (Bitmead et al., 1986). Thus, the short-time DFT can be obtained by using the following simplified state-space representation

$$\mathbf{x}(k+1) = \mathbf{A}\mathbf{x}(k) \quad (4)$$

$$y(k) = \mathbf{C}^T \mathbf{x}(k)$$

where the matrices  $\mathbf{A}$  and  $\mathbf{C}^T$  for the  $n$ th frequency component  $\omega_n$  are written as

$$\mathbf{A}_n = \begin{bmatrix} 1 & 0 & 0 \\ 0 & \cos(T_s \omega_n) & \sin(T_s \omega_n) \\ 0 & -\sin(T_s \omega_n) & \cos(T_s \omega_n) \end{bmatrix} \quad (5)$$

$$\mathbf{C}_n = [1 \quad 1 \quad 0] \quad (6)$$

Table 1: Parameters of reference systems

Parameters	Ref. system A	Ref. system B
$K$ [N/m]	$5.75 \cdot 10^4$	$3.10 \cdot 10^4$
$D$ [Ns/m]	100	90
$J_1$ [kgm <sup>2</sup> ]	0.032	0.032
$J_2$ [kgm <sup>2</sup> ]	0.032	0.032
$f_{res}$ [Hz]	15.1	11.1

where  $T_s$  is the sample time. Thus, the state vector consists of the DC offset and the real and imaginary components of the signal at the frequency  $\omega_n$ , and it is described by

$$\begin{bmatrix} x_{dc}(k+1) \\ x_{re}(k+1) \\ x_{im}(k+1) \end{bmatrix} = \begin{bmatrix} 1 & 0 & 0 \\ 0 & \cos(T_s \omega_n) & \sin(T_s \omega_n) \\ 0 & -\sin(T_s \omega_n) & \cos(T_s \omega_n) \end{bmatrix} \begin{bmatrix} x_{dc}(k) \\ x_{re}(k) \\ x_{im}(k) \end{bmatrix} \quad (7)$$

The equation for the output is given as

$$y(k) = [1 \quad 1 \quad 0] \begin{bmatrix} x_{dc}(k) \\ x_{re}(k) \\ x_{im}(k) \end{bmatrix} \quad (8)$$

The second and third element of the state vector  $\mathbf{x}(k)$  consist of a frequency component and its derivative. Thus, the output  $y(k)$  formed from the real part of the signal components. The Kalman filter solution for the state estimation problem can be written as

$$\hat{\mathbf{x}}(k+1) = \mathbf{A}\hat{\mathbf{x}}(k) + \mathbf{K}(k)(y(k) - \mathbf{C}^T \hat{\mathbf{x}}(k)) \quad (9)$$

where  $y(k)$  is the measured signal and the Kalman gain  $\mathbf{K}(k)$

$$\mathbf{K}(k) = \frac{\mathbf{A}\mathbf{P}(k)\mathbf{C}^T}{\mathbf{C}^T \mathbf{P}(k)\mathbf{C} + r} \quad (10)$$

where  $r$  represents variance in the measurement. The covariance matrix  $\mathbf{P}(k)$  is calculated as

$$\mathbf{P}(k) = \mathbf{A}\mathbf{P}(k-1) \left[ \mathbf{I} + \frac{\mathbf{C}\mathbf{C}^T \mathbf{P}(k-1)}{\mathbf{C}^T \mathbf{P}(k-1)\mathbf{C} + r} \right] \mathbf{A}^T \quad (11)$$

As the covariance matrix is updated, the optimal gain has a time-varying nature. For practical purposes, fixing the covariance matrix at  $\mathbf{P} = \epsilon \mathbf{I}$  gives the steady-state values of the Kalman gain vector, which can be calculated offline as

$$\mathbf{K}(k) = \frac{\mathbf{A}\mathbf{C}}{\mathbf{C}^T \mathbf{C} + \frac{r}{\epsilon}} \quad (12)$$

This expression gives a filter expression that is a fixed coefficient state observer with predetermined stability characteristics (Kamwa et al., 2014). Furthermore, this

form gives a simple tuning rule for the gain: the gain only depends on the ratio  $r/\epsilon$  as the known matrices  $\mathbf{A}$  and  $\mathbf{C}$  are calculated beforehand. Thus, the choice of  $\epsilon$  directly influences the tracking and error covariance; for instance, a small value gives slow tracking and a small error covariance. The ratio of  $r$  and  $\epsilon$  is defined as

$$\lambda = \frac{r}{\epsilon} \quad (13)$$

This form provides an opportunity to use only one tuning parameter  $\lambda$  in the filter design. The state-space realization can be modified so that more than one frequency component can be considered at the same time by using the block-diagonal representation

$$\mathbf{A} = \begin{bmatrix} \mathbf{A}_1 & 0 & 0 & 0 \\ 0 & \mathbf{A}_2 & 0 & 0 \\ 0 & 0 & \ddots & 0 \\ 0 & 0 & 0 & \mathbf{A}_n \end{bmatrix} \quad (14)$$

and correspondingly, the output matrix has the form

$$\mathbf{C}^T = [1 \ 0 \ 1 \ 0 \cdots \ 1 \ 0] \quad (15)$$

As the signal is in a complex form, the amplitude of the  $n$ th component can be calculated by

$$|x^{(n)}| = \sqrt{x_{\text{re}}^{(n)} + x_{\text{im}}^{(n)}} \quad (16)$$

### 3.1 Estimating with Short-time DFT

In order to show the tracking properties and the influence of the tuning parameters of the Kalman filter, the following signal is considered as an example

$$y(t) = 2 + 1.3 \sin(30\pi t) + 1.7 \sin(80\pi t) + e(t) \quad (17)$$

where  $e(t)$  is the disturbance in the signal that consists of a Gaussian noise part and three sine components with frequencies  $[26, 54, 72]\pi$ . The amplitude for the disturbance is set to 0.25. The Kalman filter is tuned to track frequencies  $\omega_{1-7} = [20, 24, 30, 36, 60, 70, 80]\pi$  that include both the sine components of the signal (17) and the other components close to the disturbance frequencies. Figure 2 a) shows the estimated amplitudes for the frequencies  $\omega_{1-7}$ . Moreover, Figure 2 b) depicts the tracking properties in the case of a second sine component of (17) when the tuning parameter  $\lambda$  is varied. It can be noticed in Figure 2 a) that the amplitudes of the desired frequency components of (17) are estimated correctly under disturbances. Furthermore, the amplitudes of the other frequencies considered in the Kalman filter design as well as in  $e(t)$  are estimated near zero. In Figure 2 b), the effect of the

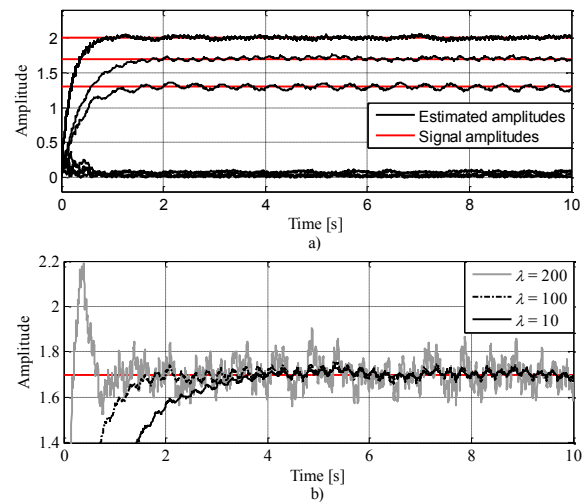


Figure 2: a) Estimated amplitudes of the signal ( $\lambda = 100$ ) and b) tracking properties when the tuning parameter  $\lambda$  is varied.

tuning parameter  $\lambda$  is clear: when  $\lambda$  increases, the error in the estimate increases, but the tracking is faster. These results show that the desired frequency components can be tracked by the proposed method.

## 4 Experimental Results

In the experimental evaluation, a mechanical system consisting of two nip rollers coupled by a flexible belt is considered. Both of the rollers are directly coupled to BSM100N-2250AD permanent magnet synchronous motors manufactured by Baldor. The motors are controlled with high-performance ABB ACSM1 frequency converters. The velocity feedback signals are measured using high-resolution absolute encoders. An AC500 programmable logic controller (PLC) by ABB is used to implement the process controllers and the excitation signals. The experimental test setup is illustrated in Figure 3.

### 4.1 Offline Identification

In this paper, the offline identification is considered for two specific purposes. Firstly, based on the offline identification results, the desired set of frequency points to be monitored by the online method are selected, and thus, the frequency contents of the excitation signal are obtained. Secondly, the dynamics of the experimental system is identified in order to have a more realistic model for comparison.

The experimental offline identification tests are carried out in the nominal operation point of the system at a velocity of 10rad/s when the belt tension was set



Figure 3: a) Experimental system applied in the laboratory measurements. Both of the rollers are driven by Baldor BSM100N-2250AD permanent magnet synchronous motors and controlled by ABB ACSM1 frequency converters

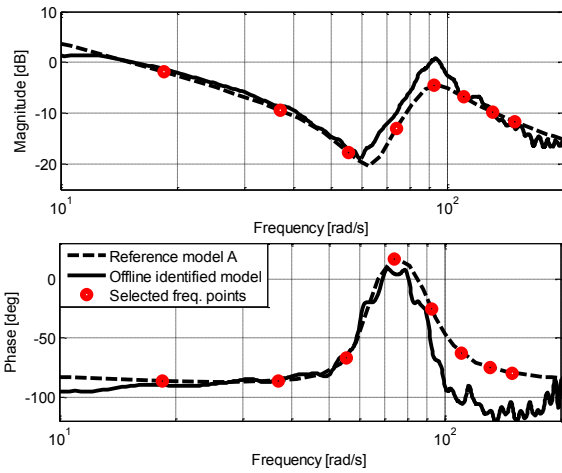


Figure 4: a) Offline-identified phase and magnitude response compared with the mathematical model (reference model A). The red dots are the selected frequencies to be monitored by the proposed online method.

to 50 N. The identification of the controlled system is carried out so that the system dynamics is excited with a pseudo random binary signal (PRBS) with 7-register and amplitude changes between the values -2.3 Nm and 2.3 Nm. The velocity is controlled by a closed-loop PI control, and the excitation signal is added to the output of the controller. By using a low-bandwidth controller, the system dynamics can be identified without losing principal information (Villwock and Pacas, 2008), (Garrido and Concha, 2013), (Garrido and Concha, 2014). In Figure 4, the experimentally identified phase and magnitude responses are compared with the frequency response of reference model A of Table 1. The offline-estimated nonparametric model is in a satisfactory agreement with the reference two-mass model. Even though there are small discrepancies between

the models, the characteristics of the two-mass-system are evident in the measured phase and magnitude responses. It is pointed out that the direct comparison of the offline-identified model with the reference model of the mechanical system is difficult as the original parameters are only known with some degree of confidence. Nevertheless, the identification result is in a satisfactory agreement with the mathematical model.

As stated above, for online identification purposes, the monitoring of the mechanical system at a selected set of frequencies is a desirable feature. Based on the a priori assumption of the system dynamics and the offline identification result, the selected frequency points to be monitored are illustrated by red dots in Figure 4. The selected set includes eight frequency components close to the resonance frequency from 2.9 Hz to 23.9 Hz with a frequency resolution of 3Hz.

## 4.2 Estimation of Measured Output

Periodic signals are considered in this paper with  $N_p$  samples in the period, and in particular, with a random phase multisine signal, which can be written as

$$r_u(t) = \sum_{n=1}^{N_f} A_k \cos(2\pi f_k t + \phi_k) \quad (18)$$

where  $N_f$  is the number of frequencies,  $A_k$  are the amplitudes of each frequency component,  $f_k$  are the frequencies chosen from the grid  $\frac{2\pi l}{N_p}, l=1, \dots, \frac{N_p}{2}-1$  and random phases uniformly at an interval between 0 and  $2\pi$ . The signal contains frequencies in the frequency range of 2.9 to 23.9 Hz with the frequency resolution of 3 Hz, and the amplitudes are chosen as one. The frequency response is only estimated at the excited frequencies. Figure 5 e) shows an example of a multisine signal amplitude in the frequency domain.

In order to illustrate the short-time DFT for online identification, the system is first excited with a different multisine excitation signal as illustrated in Figure 5. As the output of the Kalman filter is formed from the estimated states (8), it represents an estimation of the measured signal  $y(k)$  calculated from the DC offset and real components. Similar type of an estimation problem for identifying the amplitudes of a harmonic signal has been considered in (San-Millan and Feliu, 2015). In this paper, the estimation properties of the Kalman filter are considered in the case of measured velocity. It is worth mentioning that the amplitude of the excitation signal has been intentionally set high for illustrative purposes. In Figure 5 a)-d), the measured velocity is compared with the estimated output. The excitation signal contains different frequencies as depicted in Figure 5 e). In Figure 5 a), the system is excited with an excitation signal with

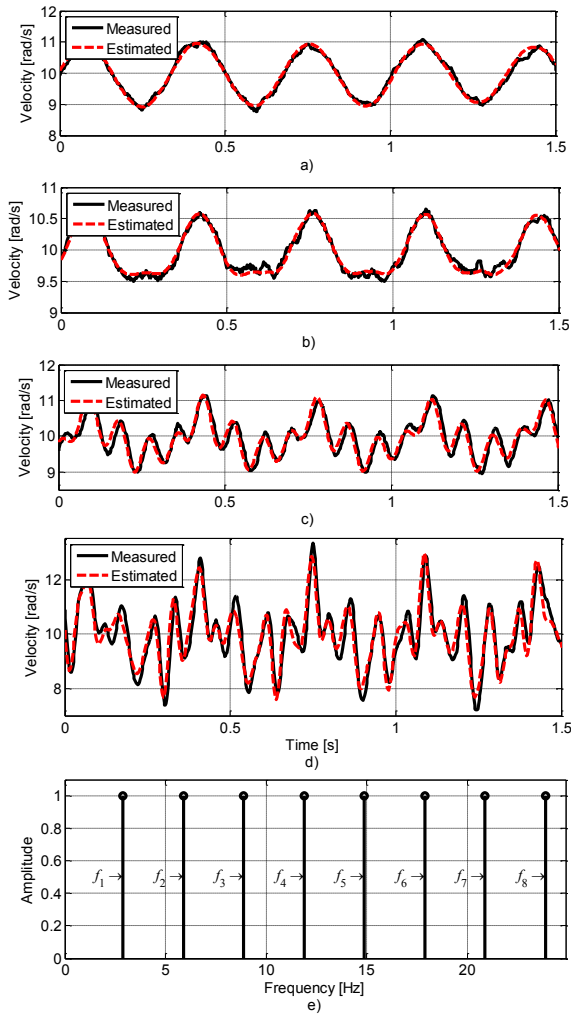


Figure 5: Estimated velocity compared with the measured velocity. a) The system is excited with  $f_1$ , b) with  $f_1$  and  $f_2$ , c) with  $f_1$ - $f_4$ , and d) with  $f_1$ - $f_8$ . e) The frequency contents of the multisine signal with a frequency range of 2.9 Hz to 23.9 Hz with a frequency resolution of 3Hz.

only one frequency  $f_1$ , in Figure 5 b) with two frequencies  $f_1$  and  $f_2$ , Figure 5 c) with four frequencies  $f_1$ - $f_4$ , and in Figure 5 d) with eight frequencies  $f_1$ - $f_8$ .

It can be seen in Figure 5 that the estimated signals are in a satisfactory agreement with the measured signal. Especially, in the cases a)-c), there are only slight discrepancies between the signals caused by the noise in the measurement and the small eccentricity of the roller. In Figure 5 d), the largest estimation error can be detected in the case when the excitation signal contains more frequencies; nevertheless, the estimated signal behavior agrees well with the measured one. As a conclusion, the excited frequencies can be clearly ob-

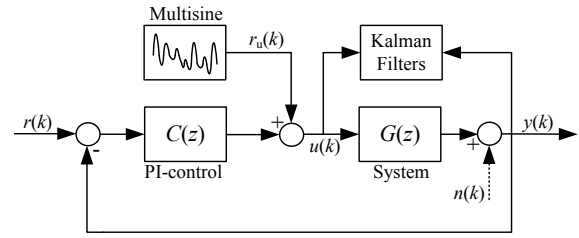


Figure 6: Scheme of the closed-loop identification.

served with the Kalman filter, thus indicating that the short-time DFT can be obtained.

### 4.3 Online Identification

First, the experimental test setup with reference parameters A (see Table 1) is considered. The system is excited with a multisine signal as depicted in Figure 5 e). The velocity is controlled with a low bandwidth PI controller, and the online estimation is performed directly by using the measured input  $u(k)$  and the output signals  $y(k)$  by Kalman filters as illustrated in Figure 6. The tuning parameter of the Kalman gain is chosen as  $\lambda = 100$ . It is pointed out that the effect of the feedback controller is now omitted as a low-bandwidth controller is used. By using (16), the amplitudes of the desired frequencies can be calculated. Thus, the ratio of the output magnitudes to the input magnitudes can be used for the estimation of the frequency response at the excited frequencies. In Figure 7, the online-estimated frequency response points are compared with the frequency responses of the offline-identified model and the reference model. Although there are slight differences between the reference frequency response and the estimated frequency points, the form of the resonance frequency can be clearly seen from the online estimated result. However, the online estimation result shows similar behavior as the offline-identified frequency re-

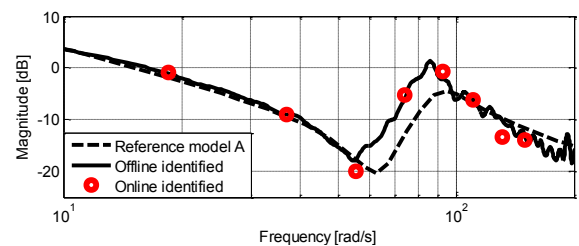


Figure 7: Online-identified frequency response points compared with the frequency response of reference model A and the offline-identified model. The red dots are the identified points with the proposed online method.

sponse, as it was expected. Moreover, we can see that the frequency component  $f_7$  has the largest error compared with the reference and offline-identified models. However, these results are not directly comparable because of the fundamental difference between the excitation signals and the estimation methods. Nevertheless, the online estimation result is in a good agreement with the offline-identified model. Evidently, the online-identified nonparametric models in different frequency points describe the system behavior and validate the accuracy of the proposed estimation method.

#### 4.4 Changes in the System Dynamics

The results in Figure 7 show that the dynamics of the two-mass system in the chosen frequency points can be identified directly by using Kalman filters that perform like a Fourier transform. In order to further verify the online method, the system dynamics of the experimental test setup is varied by changing the belt material between the rollers. Thus, in this paper, the modified system is regarded as reference system B with a different resonance frequency (see Table 1). In Figure 8, the online-estimated frequency points of both systems are compared with the offline-identified frequency responses. It can be observed in Figure 8 that the dynamics of the system has changed. Even though the change is small, it is enough to demonstrate that the resonance of the system has changed, which can be clearly noticed from the offline-identified frequency responses. More importantly, the same change can also be observed from the online-estimated frequency points. Especially, the change can be seen from the frequency points  $f_3$  and  $f_4$  that are close to the resonance and antiresonance frequencies of both systems. Furthermore, it can be noticed that the online-identified frequency component  $f_7$  has the largest error compared with the offline-identified model in both magnitude response results. Moreover, the online-identified phase responses show more error compared with the offline-identified ones. Nevertheless, the online-identified results are in a satisfactory agreement with the offline-identified ones, thereby indicating that the short-time DFT can be applied to online identification. The characteristics of the two-mass system are evident in the online-identified amplitude and phase responses.

#### 4.5 Distance Between the Identified Models

Typically, in order to measure the distance between the transfer function models of linear time invariant (LTI) systems, different gap metrics are used. The Vinnicombe metric (v-gap metric) between two plants

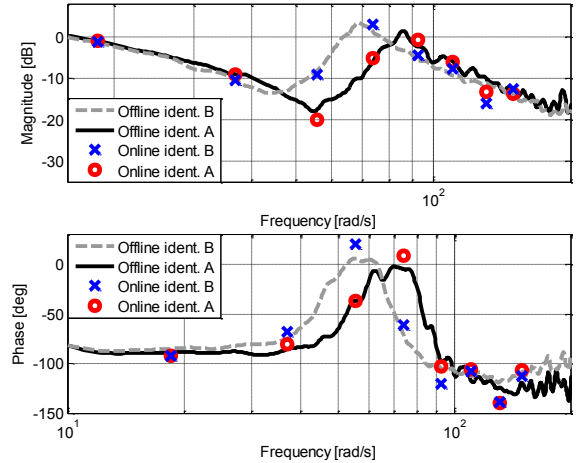


Figure 8: Online-identified frequency response points when the system is changed. The black solid line represents offline-identified system A and the dashed line system B.

$G_A(j\omega)$  and  $G_B(j\omega)$  is defined by (Vinnicombe, 1993)

$$\Psi[G_A, G_B] = \frac{|G_A(j\omega) - G_B(j\omega)|}{(1 + |G_A(j\omega)|^2)^{\frac{1}{2}}(1 + |G_B(j\omega)|^2)^{\frac{1}{2}}} \quad (19)$$

The v-gap distance is determined as

$$\delta_v(G_A, G_B) = \|G_A(j\omega), G_B(j\omega)\|_{\infty} \quad (20)$$

for the frequencies  $0 \leq \omega \leq \pi f_s$  with the normalized limits  $0 \leq \delta_v < 1$ . In other words, a frequency-based comparison of two systems can be obtained. By considering a known controller  $C(j\omega)$  and a system model  $G(j\omega)$ , a complementary sensitivity function can be written

$$T(j\omega) = \frac{G(j\omega)C(j\omega)}{1 + G(j\omega)C(j\omega)} \quad (21)$$

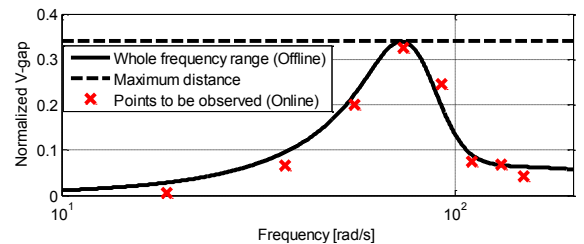


Figure 9: Frequency-based Vinnicombe gap. The solid black line is the distance of the offline-identified system models, and the dashed line is the maximum distance between them. The distances of the online-identified models at a selected set of frequencies are indicated by crosses.

In general, the v-gap metric can be used to compare the stability conditions of a controller designed for a certain plant against a set of system models. However, in this paper, the v-gap metric is only used as an illustrative distance metric in order to compare offline- and online-identified models when the system has been changed. The solid black line in Figure 9 illustrates the frequency-based v-gap of the of system models that are built from the known controller and the offline-identified model (21). It can be seen in Figure 9 that the change in the distance between the systems is noticeable as the gap of the systems is higher in the frequency region near the resonances. Furthermore, it can be noticed that the frequency region after the resonance has a small gap between the systems. In practice, this shows that there is uncertainty in the identification. Thus, in the case of parametric identification of two-mass system dynamics, this would correspond to an error in the inertial parameters. Nevertheless, the distance metric clearly shows the system changes when the resonance of the system is varied. The online frequency domain identification yields nonparametric models in the form of  $G(j\omega_n)$  at a selected set of frequencies, thereby leading to an option to monitor system changes in the desired frequency points. In Figure 9, the same distance metrics have been calculated for the online-identified nonparametric models similarly as in the case of the offline-identified ones. It can be observed in Figure 9 that the distance calculated by using online-identified frequency points indicates the same change in the dynamics as the offline result. More importantly, even though the online-identified frequency response in Figure 8 shows some error in different points, the distance of these points in Figure 9 is in a good agreement. Moreover, the advantage of the online frequency domain identification is the nonparametric model form that can be used, without loss of generality, to monitor changes in desired frequency points rather than within the whole frequency range. However, the Vinnicombe gap can be problematic distance metric, especially when considering robust controller design for system with resonances, because large distance is easily formed from the differences in the resonances. On the other hand, using the gap-metric as an online change indicator in interesting frequency points such as -3 dB closed-loop bandwidth point could lead to possibility of monitor changes of control performance.

## 5 Conclusions

In this paper, an online nonparametric frequency domain identification method has been presented that can be used to monitor a mechanical system at a selected

set of frequencies. It is based on a Kalman filter that performs like a Fourier transform. By using the a priori knowledge of the expected frequency range, the filter can be tuned in advance to track the desired frequency components. The method was verified by experimental measurements, which confirmed the applicability of the proposed method. The results were validated by comparing the offline-identified frequency response and the online-identified frequency points. Furthermore, the experimental test setup was changed to further verify the method with different resonances. The results show acceptable agreement, thus indicating that the proposed method is suitable for the online frequency domain nonparametric identification of a mechanical system. The future work will focus on the closed-loop identification with special reference to the influence of the controller and noise on the estimation result. Moreover, by considering the adaptive form in the proposed Kalman filter, the identification could be carried out with different excitation signals for instance with a sine sweep, thereby providing the opportunity to use a simple state-space form for one frequency component.

## References

- Barkley, A. and Santi, E. Improved online identification of a dc-dc converter and its control loop gain using cross-correlation methods. *IEEE Trans. on Power. Elect.*, 2009. 24(8):2021–2031. doi:[10.1109/TPEL.2009.2020588](https://doi.org/10.1109/TPEL.2009.2020588).
- Beck, H.-P. and Turschner, D. Commissioning of a state controlled high powered electrical drive using evolutionary algorithms. *IEEE/ASME Trans. Mechatronics*, 2001. 6(2):149–154. doi:[10.1109/3516.928729](https://doi.org/10.1109/3516.928729).
- Beineke, S., Wertz, H., Schütte, F., Grotstollen, H., and Fröhleke, N. Identification of nonlinear two-mass systems for self-commissioning speed control of electrical drives. in *Proc. IEEE IECON*, 1998. pages 2251–2256. doi:[10.1109/IECON.1998.724071](https://doi.org/10.1109/IECON.1998.724071).
- Bitmead, R., Tsoi, A. C., and Parker, P. J. A kalman filtering approach to short-time fourier analysis. *IEEE Trans. Acoust., Speech, Signal Process*, 1986. 34(6):1493–1501. doi:[10.1109/TASSP.1986.1164989](https://doi.org/10.1109/TASSP.1986.1164989).
- Calvini, M., Carpita, M., Formentini, A., and Marchesoni, M. Pso-based self-commissioning of electrical motor drives. *IEEE Trans. Ind. Electron*, 2015. 62(2):768–776. doi:[10.1109/TIE.2014.2349478](https://doi.org/10.1109/TIE.2014.2349478).
- Garrido, R. and Concha, A. An algebraic recursive method for parameter identification of a servo model. *IEEE/ASME*

- Trans. Mechatronics*, 2013. 18(5):1572–1580. doi:[10.1109/TMECH.2012.2208197](https://doi.org/10.1109/TMECH.2012.2208197).
- Garrido, R. and Concha, A. Inertia and friction estimation of a velocity-controlled servo using position measurements. *IEEE Trans. Ind. Electron.*, 2014. 61(9):4759–4770. doi:[10.1109/TIE.2013.2293692](https://doi.org/10.1109/TIE.2013.2293692).
- Jenssen, A. and Zarrop, M. Frequency domain change detection in closed loop. in *Proc. Int. Conf. in Control*, 1994. pages 676–680. doi:[10.1049/cp:19940213](https://doi.org/10.1049/cp:19940213).
- Kamwa, I., Samantaray, S. R., and Joos, G. Wide frequency range adaptive phasor and frequency pmu algorithms. *IEEE Trans. Smart Grid.*, 2014. 5(2):569–579. doi:[10.1109/TSG.2013.2264536](https://doi.org/10.1109/TSG.2013.2264536).
- Kurita, Y., Hashimoto, T., and Ishida, Y. An application of time delay estimation by anns to frequency domain i-pd controller. in *Proc. Int. Joint Conf. on Neural Networks*, 1999. pages 2164–2167. doi:[10.1109/IJCNN.1999.832723](https://doi.org/10.1109/IJCNN.1999.832723).
- LaMaire, R., Valavani, L., Athans, M., and Gunter, S. A frequency-domain estimator for use in adaptive control systems. in *Proc. American Control Conf.*, 1987. pages 238–244.
- Morelli, E. A. Real-time parameter estimation in frequency domain. *Jour. of Guidance, Contr. and Dynamics*, 2000. 23(5):812–818.
- Nevaranta, N., Niemelä, M., Lindh, T., Pyrhönen, O., and Pyrhönen, J. Position controller tuning of an intermittent web transport system using off-line identification. in *Proc. EPE*, 2013. pages 1–9. doi:[10.1109/EPE.2013.6631785](https://doi.org/10.1109/EPE.2013.6631785).
- Nevaranta, N., Parkkinen, J., Niemelä, M., Lindh, T., Pyrhönen, O., and Pyrhönen, J. Online estimation of linear tooth-belt drive system parameters. *IEEE Trans. Ind. Electron.*, 2015. 0(0):1–10. doi:[10.1109/TIE.2015.2432103](https://doi.org/10.1109/TIE.2015.2432103).
- Ruderman, M. Tracking control of motor drives using feedforward friction observer. *IEEE Trans. Ind. Electron.*, 2014. 61(7):3727–3735. doi:[10.1109/TIE.2013.2264786](https://doi.org/10.1109/TIE.2013.2264786).
- Saarakkala, S. and Hinkkanen, M. Identification of two-mass mechanical systems in closed-loop speed control. in *Proc. IEEE IECON*, 2013. pages 2905–2910. doi:[10.1109/IECON.2013.6699592](https://doi.org/10.1109/IECON.2013.6699592).
- San-Millan, A. and Feliu, V. A fast online estimator of the two main vibration modes of flexible structures from biased and noisy measurements. *IEEE/ASME Trans. Mechatronics*, 2015. 20(1):93–104. doi:[10.1109/TMECH.2014.2304302](https://doi.org/10.1109/TMECH.2014.2304302).
- Toth, R., Laurain, V., Gilson, M., and Garnier, H. Instrumental variable scheme for closed-loop lpv model identification. *Automatica*, 2012. 48(9):2314–2320. doi:[10.1016/j.automatica.2012.06.037](https://doi.org/10.1016/j.automatica.2012.06.037).
- Villwock, S. and Pacas, M. Application of the welch method for the identification of two- and three-mass-systems. *IEEE Trans. Ind. Electron.*, 2008. 55(1):457–466. doi:[10.1109/TIE.2007.909753](https://doi.org/10.1109/TIE.2007.909753).
- Vinnicombe, G. Frequency domain uncertainty and the graph topology. *IEEE Trans. Automatic Cont.*, 1993. 38(9):1371–1383. doi:[10.1109/9.237648](https://doi.org/10.1109/9.237648).
- Wang, Z., Zou, Q., Faidley, L., and Kim, G. Y. Dynamics compensation and rapid resonance identification in ultrasonic-vibration-assisted micro-forming system using magnetostrictive actuator. *IEEE/ASME Trans. Mechatronics*, 2011. 16(3):489–497. doi:[10.1109/TMECH.2011.2116032](https://doi.org/10.1109/TMECH.2011.2116032).